Phys. Status Solidi B **246**, No. 7, 1496–1503 (2009) / **DOI** 10.1002/pssb.200945126

physica status solidi b
www.pss-b.com
basic solid state physics

Fission processes following core level excitation in *closo*-1,2-orthocarborane

E. Rühl[*,1], A. P. Hitchcock[2], J. D. Bozek[3], T. Tyliszczak[4], A. L. D. Kilcoyne[4], D. N. McIlroy[5], A. Knop-Gericke[6], and P. A. Dowben[7]

[1] Physikalische Chemie, Freie Universität Berlin, Takustr. 3, 14195 Berlin, Germany
[2] Department of Chemistry, McMaster University, Hamilton, Ontario, L8S 4M1, Canada
[3] Stanford Linear Accelerator, LCLS Project, 2575 Sand Hill Road, Menlo Park, CA 94025, USA
[4] Advanced Light Source, Lawrence-Berkeley Laboratory, Berkeley, CA 91420, USA
[5] Department of Physics, Engineering and Physics Bldg., University of Idaho, Moscow, ID 83844-0903, USA
[6] Fritz-Haber-Institut der Max-Planck-Gesellschaft, Faradayweg 4–6, 14195 Berlin, Germany
[7] Department of Physics and Astronomy, and the Nebraska Center for Materials and Nanoscience, University of Nebraska, Lincoln, NE 68588-0111, USA

Received 4 March 2009, accepted 13 May 2009
Published online 26 June 2009

PACS 32.80.Fb, 52.25.Jm, 82.30.Lp, 82.80.Rt

[*] Corresponding author: e-mail ruehl@chemie.fu-berlin.de, Phone: +49 30 8385 2396, Fax: +49 30 8385 2717

Time-of-flight mass analysis with multi-stop coincidence detection was used to study the multi-cation ionic fragmentation of the *closo* carborane cage molecule *closo*-1,2-orthocarborane ($C_2B_{10}H_{12}$) following inner-shell excitation in or above the B 1s regime. Electron ion coincidence spectra reveal the cationic products which are formed after core level excitation. Distinct changes in fragmentation pattern are observed as a function of excitation energy. Photoelectron–photoion–photoion coincidence (PEPIPICO) spectroscopy was used to study the dominant fission routes in the core level excitation regime. Series of ion pairs are identified, where asymmetric fission dominates, leading to ion pairs of different mass. Suitable fission and fragmentation mechanisms are discussed.

1 Introduction There has been a resurgence of interest in carborane chemistry. Although discovered in 1963 and followed quickly by a flurry of functionalization chemistry [1], the resurgence of interest in *closo*-1,2-dicarbadodecaborane (orthocarborane, Fig. 1) has been to some extent driven by the fact that this molecule is an excellent source for the fabrication of a semiconducting boron carbide [2–10], a material suitable for the fabrication of solid state neutron detectors [3–9].

The method of choice, at present, for making semiconducting boron carbides is to use *closo*-1,2-dicarbadodecaborane (orthocarborane) as a source gas in a plasma enhanced chemical vapor deposition (PECVD) for preparation of a semiconducting thin film. The resulting boron carbides, of approximate stoichiometry "$C_2B_{10}H_x$" (where x represents up to ~5 to 40% molar fraction of hydrogen [11]), exhibit a range of electronic properties suggesting that decomposition of the *closo*-carboranes, to form the "$C_2B_{10}H_x$" boron carbide semiconductor does not result in complete fragmentation of the icosahedral cage. We know that plasma enhanced or thin film deposition using the source gases of orthocarborane [2–10], the combination pentaborane (B_5H_9) and methane [10, 12], or decaborane ($B_{10}H_{14}$) combined with methane all successfully yield semiconducting boron carbide of high resistivity, whereas the *nido*-2,3-diethyl-2,3-dicarbahexaborane carborane cluster molecule does not [13].

Although the structural polytypes of semiconducting boron carbides have not, as yet, been uniquely identified, the current belief within the semiconducting boron carbide device community is that the 12 atom icosahedral cage is the key building block of a quality (device grade) boron carbide semiconductor, although it is clear that metal dopants can be introduced into the cage, substituting for one of the 12 cage atoms [14]. Excessive fragmentation would thus lead to a different boron carbide, perhaps with-

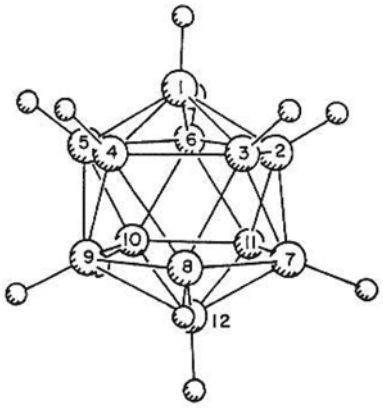

Figure 1 A schematic structure of *closo*-1,2-orthocarborane (1,2-$C_2B_{10}H_{12}$), where at two neighboring sites BH is substituted by CH.

out the high bulk resistivities characteristic of the semiconducting boron carbides, but with, perhaps, a greater material hardness.

Controlled fragmentation of *closo*-1,2-orthocarborane has been studied in the past in order to understand the fragmentation mechanisms of the singly charged molecules [15]. Complementary work on core level excitation has been communicated before, where the local electronic structure of *closo*-1,2-orthocarborane was discussed together with model calculations [16]. This is the motivation for the present work, where we report results on the fission mechanisms of core-excited *closo*-1,2-orthocarboranes. Above the B 1s core threshold fragmentation of the *closo*-1,2-orthocarborane occurs beyond just the simple loss of the exopolyhedral hydrogen, but as we show in the present work, this fragmentation into ion pairs does have favored pathways.

It is well-known that dissociative double ionization is a major ionic decay route of core excited molecules and clusters [17–21]. For understanding the fission pathways, which might be of importance to semiconducting film formation, it is important to be able to identify the cation pair formation processes. This can be done by measuring correlated ion pairs via coincidence spectroscopies, which mostly rely on time-of-flight mass spectrometry. This includes photoion–photoion coincidences (PIPICO), where the flight time difference between correlated fragment ions is measured [18, 19, 22]. For large molecules and clusters with a rich mass spectrum producing numerous mass lines by dissociative channels, PIPICO spectra are often difficult to assign. This is due to blended mass lines of the same time-of-flight differences [18, 19, 22]. For these systems, the use of a multi-stop coincidence detection technique permits the identification of individual cation flight times rather than simply differences in flight time. We have used in this work multi-stop time-to-digital detection systems to measure photoelectron–photoion–photoion coincidence (PEPIPICO) spectra, also known as charge separation mass spectrometry (CSMS) [17, 20, 23–25].

2 Experimental details The orthocarborane (i.e. *closo*-1,2-dicarbadodecaborane or 1,2-$C_2B_{10}H_{12}$) was purchased from either Katchem or Aldrich or prepared using the procedures described in Ref. [15, 16]. The identity and purity of all compounds were determined by nuclear magnetic resonance (NMR), infrared spectroscopy (IR), and mass spectral measurements and compared with literature values. NMR spectra were obtained on a Bruker AVANCE400 operating at ^{1}H 400.1 MHz, ^{13}C 100.6 MHz, ^{11}B 128.38 MHz. Proton and carbon spectra were referenced to solvent, boron spectra to an insert of $BF_3 \cdot Et_2O$.

The time-of-flight mass spectrometer consisted of a two stage acceleration region separated by grids, followed by a 30 cm drift tube. Wiley-McLaren focusing conditions were used [19, 26]. A –250 V/cm or –300 V/cm extraction field was used for the ions. Under these conditions, splitting was not detected for any of the mass peaks, indicating there was negligible distortion of the yields due to loss of high kinetic energy ions and mass discrimination.

The mass spectra of carboranes are notoriously difficult to assign, since there is hydrogen loss and the boron occurs in two different isotopomers (^{10}B and ^{11}B). We use the simplifying nomenclature that X^{N+} is the parent molecule under study with the loss of N electrons, i.e. $C_2B_{10}H_{12} \cdot X^{N+}$, but where hydrogen loss from the parent cation is apparent, this is denoted by Y_{12}^{+}. This implies that all fragment units are labeled Y_n^+, where Y^+ corresponds to BH^+ or CH^+. Note that isotopic and $Y–H_x$ distributions tend to blur any such effects in carborane samples, except for the H^+ channel. The overall efficiency for ion detection is estimated to be about 15%. The start of the flight time scale was the signal from an electron accelerated by a field of +250 V/cm (for experiments at the Advanced Light Source) or +300 V/cm (for experiments taken at BESSY-I) to a channelplate or a channeltron adjacent to the ionization region.

Photoelectron-photoion-photoion coincidence (PEPIPICO) spectra were acquired using a custom built multi-stop time-to-digital converter with a time resolution of 12 nsec [17]. Alternatively, a MIPSYS fly TDC was used with 4 or 8 ns time resolution (cf. [27]). The experiments were done at the following synchrotron radiation facilities and beamlines: (i) undulator beamline 9.0.1 of the Advanced Light Source [28] and (ii) the HE-TGM-2 beamline at BESSY-I [29] were both used with almost identical electron and cation detection setups, yielding virtually identical results. In order to avoid excessive accidental coincidences and to keep the overall event rates within the capacity of the processing system, rather narrow entrance and exit slits of the soft X-ray monochromators were used – typically ~10 μm. The photon energy resolution was better than 0.1 eV FWHM at the ALS and <0.3 eV at BESSY-I.

3 Results and discussion

3.1 Double ion fragmentation of *closo*-1,2-orthocarborane Series of time-of-flight mass spectra

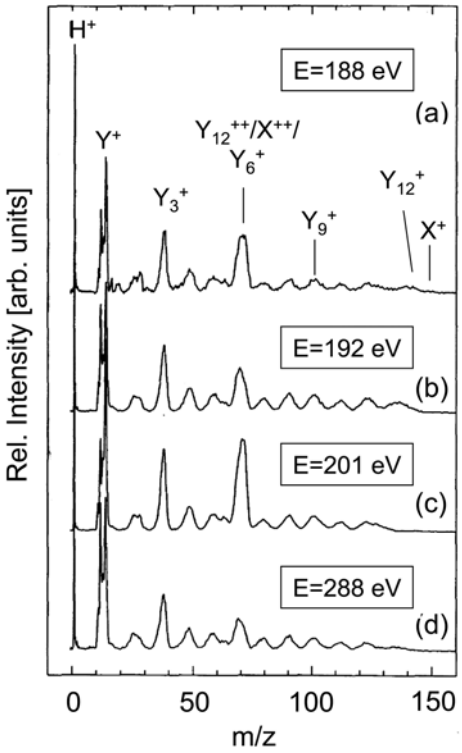

Figure 2 High extraction field time-of-flight (TOF) mass spectra of *closo*-1,2-orthocarborane, photoionized at, near, and above the B 1s threshold, as indicated. The peaks correspond to fragment ions with all possible numbers of vertices, symbolized as Y_n^+ where Y represents BH or CH. The parent cation ($C_2B_{10}H_{12}^+$) is symbolized by X^+. Note that the start signal of the time scale was taken from an any-electron detector with 250 eV/cm combined extraction field for positive ions and electrons.

are shown in Fig. 2. Figure 3 shows details of some mass ranges in greater details and improved mass resolution. Different excitation energies are shown in Fig. 2, which are below the B 1s-absortion edge (188 eV photon energy –

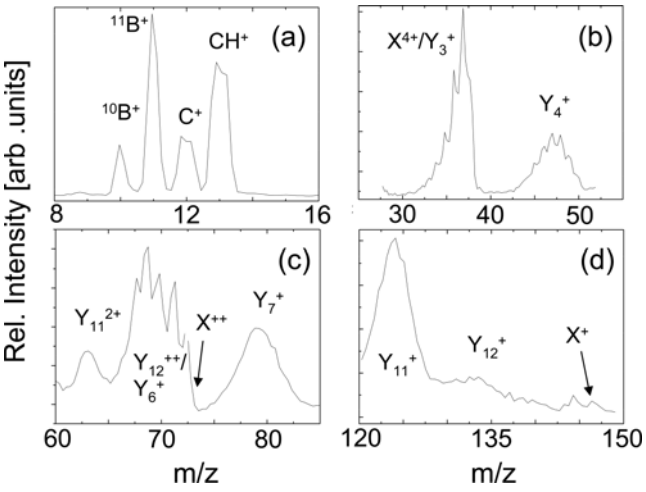

Figure 3 Detailed view on different mass ranges recorded by electron ion coincidence (PEPICO) spectroscopy at $E = 220$ eV.

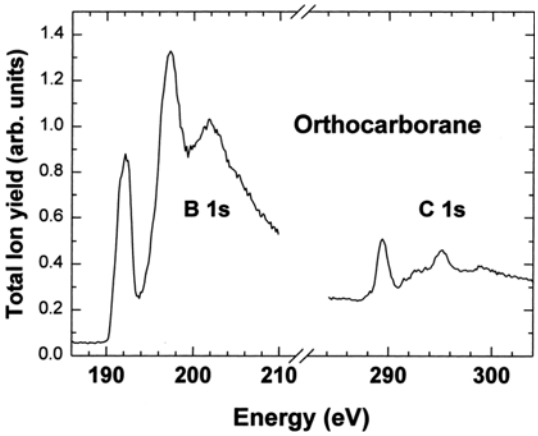

Figure 4 Total ion yield at the B 1s- and C 1s-excitation regimes for *closo*-1,2-dicarbadodecaborane: orthocarborane ($1,2\text{-}C_2B_{10}H_{12}$).

see Figs. 2(a) and 4) or above. An intense pre-edge resonance is known to occur at an incident photon energy of 192 eV (see Figs. 2(b) and 4), which is due to various B 1s to valence transitions [16]. At the photon energy of 201 eV, the B 1s electrons are emitted into the continuum (see Figs. 2(c) and 4), and 288 eV corresponds to the C 1s → 10 a″ (see Figs. 2(d) and 4), 17 a′-valence transition [16]. Figure 4 shows the total ion yield from orthocarborane in the B 1s- and C 1s-excitation regimes.

Note that the total cation yield is similar to the absorption cross section, but there are distinct differences, which are reflected in the number of ions produced per absorbed photon [18]. This production of multiple ions is known to enhance the continua relative to the absorption cross section [21], since in these regimes at least two ions are formed per absorbed photon.

The multiple ion production is a result of dissociative double ionization, which corresponds to fission and is often called "Coulomb-explosion", although, regrettably, the differences between these two processes are often ignored [30]. This is specifically applicable in the case of molecules, which typically do not form a stable molecular di-cation. Such examples include most small molecules, whereas large molecules often readily form stable di-cations [31]. The stability of the molecular di-cation is specifically true for cage-like molecules, such as C_{60}, which shows weak fragmentation [32]. Carboranes are of specific interest to efforts to understand fragmentation of cage like species, since they show both chemical fragmentation from the singly charged molecule [15] as well as stable di-cation formation [16], and are examples where the charge separation pathways are not known in detail.

Total ion yield spectra shown in Fig. 4 are plotted on the same vertical scale in order to indicate the relative absorption cross section and the importance of element-selective excitation. The pre-edge regime below the B 1s-edge exhibits weak cross section [33]. In contrast, the C 1s-edge is superimposed on an intense B 1s-continuum. Overall, this result is not surprising since the atomic ratio

between elemental boron and carbon is five in orthocarborane. Therefore, all results obtained from studies in the C 1s-regime contain a sizable background from B 1s-excitation.

All mass spectra shown in Fig. 2 are dominated by an intense H^+-signal, similar to previous work [15]. The intensity of this mass signal is used to compare the mass spectra to each other.

The intense signal Y^+ denotes the mass region of B^+ to CH^+, as shown in detail in Fig. 3(a). This mass region is clearly split into two or more mass lines, as shown in Figs. 2 and 3(a). A clear assignment based on these low mass resolution results is difficult, considering the substantial kinetic energy release which goes along with fragmentation in the core level excitation regime. The portion at lower masses is assigned to the stable isotopes of boron (^{10}B (natural abundance: 20% [34]) including possible bonding to hydrogen, whereas the high-mass portion is likely due to ^{11}B (natural abundance: 80% [34])) and BH^+. This signal is blended with C^+ ($m/z = 12$), where Fig. 3(a) indicates that $m/z = 12$ is essentially due to C^+, as follows from the ratio of the mass lines of $^{10}B^+$ and $^{11}B^+$, and the intensity of C^+ is substantially weaker than of CH^+ ($m/z = 13$).

Interestingly, the ratio between both most intense mass lines ($m/z = 11$ and 13 cf. Figs. 2 and 3(a)) is similar for all excitation energies, whereas a substantial change is observed upon C 1s excitation at 288 eV. This photon energy is located below the C 1s ionization energy, which is known to occur at 292.8 eV [16]. The similar mass peak intensity can be rationalized by the properties of the resonant C 1s→10a″, 17a′-valence excitation. Such core to valence molecular excitations lead to excited singly charged species, so that CH^+ is formed with lower probability than at other photon energies, where direct C 1s photoemission occurs or CH^+ is formed via charge or energy transfer processes, such as e.g. the intramolecular Coulombic decay (ICD) [35, 36]. This ultrafast energy transfer process has been predicted to occur in molecules and clusters, providing an efficient route to delocalize charges of a locally excited system. Such process is then followed by fission, if the internal energy is sufficient. This also indicates that the cations are most efficiently formed upon core level excitation via fission, i.e. from the doubly or multiply charged parent cation or its fragments.

There are two other prominent mass lines visible in the mass spectra shown in Figs. 2 and 3(b), (c). These are labeled Y_3^+ and Y_6^+. The assignment of the intense Y_6^+ signal is straightforward. It is essentially due to the doubly charged parent X^{++}, which also shows some loss of hydrogen yielding Y_{12}^{++}, as shown in Fig. 3(c). In contrast, the mass regime of the parent cation X^+ and Y_{12}^+ marked in Figs. 2 and 3(d) is weak in intensity and is unlike photoionization of valence electron [15]. This weak parent molecular cation production is expected since core level excitation leads to double and multiple ionization [21]. Consistent with this assignment of Y_6^+ to the di-cation Y_{12}^{++}, is the finding that the Y_6^+ signal is weaker in intensity at the resonant B 1s excitation at 192 eV (see Fig. 2(b)), where similar arguments hold as for the above mentioned variations in C^+ mass signal. This assignment of Y_6^+ to the di-cation Y_{12}^{++} is also in full agreement with the weak intensity of Y_6^+ at 288 eV (see Fig. 2(d)). In contrast, in the B 1s-continuum (201 eV), we observe a considerably more pronounced Y_6^+ signal (see Fig. 2(c)).

The other dominant mass signal is Y_3^+. There might be two different assignments for the mass signal: (i) a fragment consisting of three boron/carbon units and hydrogen; (ii) the quadruply charged parent cation (X^{4+} (or Y_{12}^{4+})). The latter possibility (a quadruply charged parent cation) may be excluded as being the dominant species, since the triply charged parent (X^{3+} (or Y_{12}^{3+})) occurring in the Y_4^+ regime is seen to be weak in intensity and quadruple ionization is expected to be weaker than triple ionization in the soft X-ray regime. It is thus straightforward to assign the major contribution to the Y_3^+ signal to a $(B/C)_3H_x^+$ fragment, peaking at $m/z = 39$. This Y_3^+ or $(B/C)_3H_x^+$ signal is likely formed from a face of the icosahedral neutral carborane cage (cf. Figure 1). Its intensity also varies with photon energy, similar to Y_6^+. Therefore, we conclude that the fragment Y_3^+ is predominantly a result of fission and removal of an icosahedral face ($(B/C)_3H_x^+$) which requires breaking fewer bonds than many other possible fission products. This point is further discussed below in the context of multicoincidence experiments. Clearly, there is weaker intensity upon resonant B 1s- and C 1s-excitation. This change in intensity also affects the other mass signals, which are seen most clearly upon resonant excitation. These come from a background of single ionization, where a broad distribution of mass lines has been found in earlier work [15]. The present results are in full agreement with Ref. [15], where the relative strength of these cations becomes more prominent in spectral regions, where single ionization dominates.

Figure 5 shows the results from PEPIPICO spectra recorded in the B 1s continuum ($E = 220$ eV). PEPIPICO spectra are sensitive to processes leading to two correlated cations, i.e. dissociative double or multiple ionization [23]. Figure 5 is recorded in a spectral regime, where Auger processes are the major process contributing to double ionization. Additional experiments were performed at various photon energies, similar to the results shown in Fig. 2.

It turns out, that the PEPIPICO spectra taken at various photon energies are similar in shape and the significant

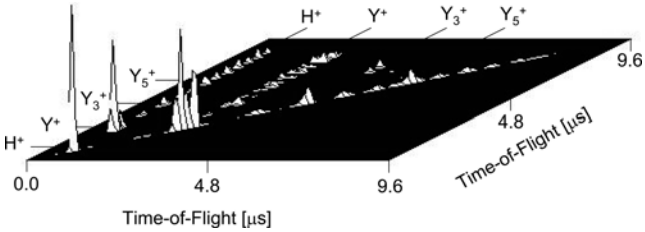

Figure 5 Photoelectron–photoion–photoion coincidence (PEPIPICO) spectrum for *closo*-1,2-dicarbadodecaborane: orthocarborane ($1,2\text{-}C_2B_{10}H_{12}$) recorded at 220 eV photon energy.

changes are only in the intensities, while the ratio between the coincidence channels remains essentially unchanged. This is in agreement with related work on molecules and clusters, where mostly changes in fission intensity are found upon variations of the excitation energy [27]. Specifically, in the pre-edge regime, where double ionization via Auger channels does not occur, the signal strength is weak and can only come from direct double ionization, i.e. the simultaneous emission of two valence electrons. This is a process that is known to be of weak cross section [37]. The relative strength of PEPIPICO signals increases significantly upon excitation of the near-edge resonance and above the B 1s ionization energy.

The symmetric fission channels are found along the diagonal of Fig. 5, where ions of the same flight time (i.e. the same *m*/*z*-values) are formed from a doubly charged precursor. These are dominant in intensity, especially the channels H^+/H^+, Y^+/Y^+ (cf. Section 3.3). Among the symmetric channels the dominant ones are due to ion pair of the light fragments, i.e. H^+/H^+ (33%), B^+/B^+(32%), CH^+/CH^+(25%), and Y_3^+/Y_3^+ (9%). This is similar to earlier work on clusters [20], but one has to keep in mind that false coincidences are present in the spectra and appear along the diagonal of the PEPIPICO-spectra, such as in Fig. 5. Contributions to false coincidences are found to be of weak intensity, since the signals on the diagonal are weak above the Y^+/Y^+-channel (see Fig. 5). Specifically, the results shown in Fig. 5 indicate, that the symmetric fission channels correspond to 40% of the fission intensity, whereas 60% are due to asymmetric fission channels. The latter process generates correlated ion pairs of different mass-to-charge-ratio. This implies that asymmetric fission routes are dominant, which is similar to earlier work on rare gas clusters [20]. The pattern of asymmetric mass fission channels observed in Fig. 5 is quite rich and the groups of cation pairs have been identified. Figure 6(a)–(d) shows regions of some selected fission channels, which are discussed in greater detail below.

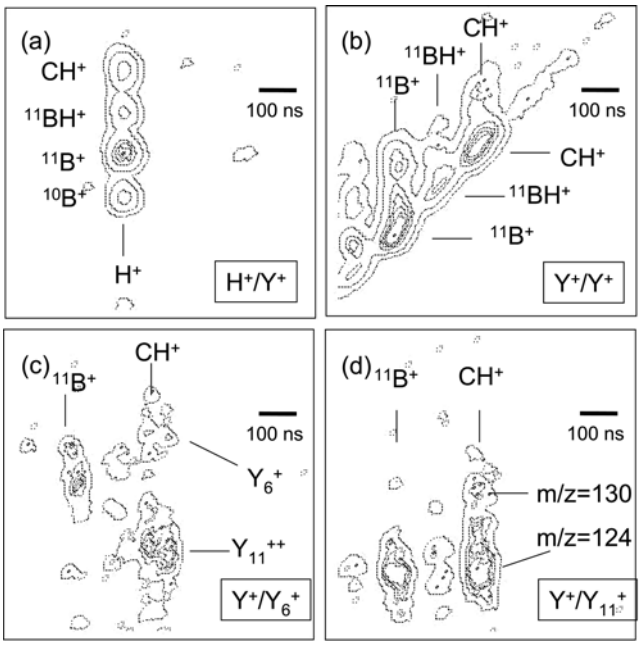

Figure 6 Detailed views represented as contour plots on sections of the photoelectron-photoion-photoion coincidence (PEPIPICO) spectrum for *closo*-1,2-dicarbadodecaborane: orthocarborane ($1,2\text{-}C_2B_{10}H_{12}$) recorded at 220 eV photon energy (Y: C^+ or B^+, X: $1,2\text{-}C_2B_{10}H_{12}^+$): (a) H^+/Y^+-regime; (b) Y^+/Y^+-regime; (c) Y^+/Y_6^+-regime; (d) Y^+/Y_{11}^+-regime.

3.2 The H^+/Y_n^+ fission channel in the photoelectron–photoion–photoion coincidence (PEPIPICO) of *closo*-1,2-orthocarborane Coincidences involving protons are one dominant channel of fission processes, corresponding to 38% of the total fission intensity. This dominant channel involving hydrogen cations is explained by the saturation of carboranes by hydrogen. The H^+ is the lighter moiety which is correlated with heavier ion production, and this reaches up to the higher mass regime of Y_{11}^+ (up to $m/z = 135$ with weak intensity). This implies that simple two body fragmentation processes are not dominant. This is unlike fission processes occurring in small molecules [23]. Evidently, more complicated processes occur in numerous fission pathways. These multiple fission pathways are more clearly distinguished by PEPIPICO spectroscopy and cannot be readily identified in the simple PIPICO spectra.

There are two intense processes involving H^+: (i) H^+/H^+ and (ii) H^+/Y^+. Their relative intensity is 12.9% and 14.4% of the total fission intensity, respectively. The other H^+/Y_n^+-channels ($n \leq 11$) are weak in intensity, with 10% of the fission intensity. The dominant H^+/Y^+-channel indicates that fission occurs upon localized excitation at one of the C- or B-sites of the cage, assuming that hydrogen is almost transparent in the B 1s- and C 1s-regime.

A local B^{++} or C^{++} leads to the correlated fragments $H^+ + B^+$, $H^+ + BH^+$, and $H^+ + CH^+$, where the former channel is dominant. The observation of these ion pairs could imply that fission occurs locally at one corner of the cage, i.e. without any charge delocalization. We will discuss further below that this appears to be unlikely, when the kinetic energy release of the fragments is considered, indicating that these come most likely from different parts of the molecule. The ratio of the signals shown in Fig. 6(a) indicates that H^+ is predominantly correlated with atomic boron (B^+), a weaker fraction of 16% leaves the BH^+ moiety intact. Coincidences involving atomic carbon yield H^+/CH^+ occur. Since the signal at $m/z = 12$ is ascribed to BH^+, caution must be used in considering the mixing ratio of both elements in the mass spectra of *closo*-1,2-orthocarborane.

We can only speculate about the fission mechanism and the size of the unseen neutral or neutrals, which cannot be investigated by PEPIPICO spectroscopy. It is known that a detailed peak shape analysis permits to derive information on the fission process as well as the neutrals that are formed before or after fission [23], but in the case of H^+-channels the analysis is difficult, since most of the ki-

netic energy is taken by the proton as the lighter moiety [24]. Figure 6(a) shows in greater detail in a contour diagram the H^+/Y^+-channels. The patterns are almost round shaped and do not permit to derive a slope of the coincidence signals. The width of the H^+/B^+-signal is 120 ± 10 ns, as derived for the PIPICO width, i.e. perpendicular to the main diagonal (corresponding to a cut through the signal at a slope of −1). The kinetic energy release (KER) would then be 3.5 ± 0.5 eV, using the results from earlier work [38]. This implies that the unseen neutral corresponds to Y_{11}. This kinetic energy release is compatible with the molecular structure of *closo*-1,2-orthocarborane ($C_2B_{10}H_{12}$), considering the bond length published earlier [16]. In a simple electrostatic picture a kinetic energy release of 3.5 ± 0.5 eV corresponds to a charge separation distance of 4.2 ± 0.6 Å. This result corresponds to the maximum charge separation in orthocarborane, if the geometry of the neutral is considered. This result may imply that the charges delocalize before fission occurs, implying that the assumed fission mechanism is correct.

3.3 The Y^+/Y_n^+ fission channel in the photoelectron–photoion–photoion coincidence (PEPIPICO) of *closo*-1,2-orthocarborane The other dominant series of cation pairs is Y^+/Y_n^+ (cf. Figs. 5 and 6(b)). It contains 42% of the fission intensity. Similar to the H^+/Y_n^+-channels, all products of the heavier moiety up to Y_{11}^+ are observed (see Fig. 6(d)). This can be explained by a process, where two corners of the icodahedron are involved in charge separation. The most dominant signal is located near the diagonal, i.e. Y^+/Y^+, where ca. 65% of the intensity of this cation pair series are located. This comes predominantly from the symmetric fission channels B^+/B^+ (47% of the Y^+/Y^+ signal) and CH^+/CH^+ (21% of the Y^+/Y^+ signal). The intense CH^+/CH^+ signal indicates that positive charges are likely trapped at carbon sites. This appears to be not explained by the ionization energies of the constituents, since both C and CH have higher ionization energies than B and BH. We can speculate that the carbon moieties are charge traps because of low lying unoccupied electronic levels, which stabilize the di-cations. The channel B^+/CH^+ is clearly identified in Fig. 6(b). It is weak (9% of the Y^+/Y^+ signal), whereas the channel BH^+/CH^+ is only observed with minor intensity (4% of the Y^+/Y^+ signal). The signal width of the B^+/CH^+-cation pair is 60 ns and the shape is fairly isotropic (see Fig. 6(b)). This indicates that the kinetic energy release (KER) is small. Assuming a mechanism similar to that used for the discussion of the H^+/B^+-signal yields a small KER of 0.2 eV. It remains speculative to consider other mechanisms which might explain this weak cation pair.

An interesting cation pair is observed in Fig. 6(c). This corresponds to the CH^+/Y_{11}^{++} channel. There is no equivalent B^+/Y_{11}^{++}-signal. Weaker intensity is found for both the B^+/Y_6^+- and CH^+/Y_6^+-signal. The CH^+/Y_{11}^{++}- signal has a slope that is −1 ± 0.1, indicating that this signal is due to dissociative triple ionization, where one charge is located at CH^+. A KER of 4.5 ± 0.5 eV is deduced from the signal width, yielding a fission distance of 3.2 ± 0.4 Å. This distance is compatible with the size of the cage of the neutral molecule and underlines that the kinetic energy release (KER) is related to the size of the molecular cage.

The cation pair regime Y^+/Y_{11}^+ contributes to 3% to the fission intensity (see Fig. 6(d)). The main signals correspond to $^{11}B^+/(m/z = 124)$ (31% of the Y^+/Y_{11}^+-intensity) and $CH^+/(m/z = 124)$ (31% of the Y^+/Y_{11}^+-intensity). The $^{11}B^+/(m/z = 124)$ is long shaped (width of 130 ± 10 ns) with a signal slope of −1 ± 0.05. This is typical for two body fission processes or deferred charge separations [23]. A kinetic energy release (KER) of 4.6 ± 0.5 eV is derived for the assumed deferred charge separation, where it is assumed that hydrogen loss occurs prior to charge separation. This KER can be explained if the charges are located at the carbon or boron sites in the icosahedron, if a maximum charge separation is considered. Figure 6(d) also indicates that other Y^+/Y_{11}^+-channels of Y_{11}^+ fragments containing more hydrogen are weak. Somewhat more intensity of such channels (involving up to $m/z = 130$) is observed for coincidences involving CH^+.

3.4 The Y_2^+ and Y_3^+ fission channels in the photoelectron–photoion–photoion coincidence (PEPIPICO) of *closo*-1,2-orthocarborane All fission processes involving Y_2^+ as a lighter moiety are weak and occur only with spurious intensity (1.5% of the fission intensity). Evidently, this cation is unstable and may undergo, if formed, a secondary loss of a neutral Y unit, contributing to the Y^+-channels.

The cation pairs containing Y_3^+ as a lighter moiety are more intense, yielding ca. 6% of the fission intensity, of which the symmetric fission dominates. As noted above, the Y_3^+ corresponds to removing a face of the icosahedral cage and breaks fewer bonds, so must be considered a likely fission route. Fission leading to ion pairs heavier than Y_3^+ as a lighter moiety are weak in intensity. This underlines that fission in orthocarborane leads to highly asymmetric product channels, if one neglects the intense symmetric product pairs H^+/H^+ and Y^+/Y^+.

4 Conclusions This study has provided coincidence time-of-flight (PEPICO and PEPIPICO) mass spectra of *closo*-1,2-orthocarborane, excited in the B 1s region, as a function of photon energy. The results reveal massive fragmentation in the inner-shell regime, where distinct changes in ion intensity are observed as the photon energy is tuned from below the B 1s-edge to the C 1s-edge. It is already evident from PEPICO experiments that double ionization modifies the coincidence mass spectra. This becomes evident from the intense di-cation mass lines Y_{12}^{++}.

Further insight into the fission channels has now been obtained from PEPIPICO experiments. It is found that symmetric fission yields mostly the light fragments H^+ and Y^+. Series of asymmetric fission are observed, where the dominant ones involve either H^+ or Y^+ as a lighter moiety.

The natural isotope abundance and loss of hydrogen do not permit to assign unequivocally the fission mechanisms. However, some selected examples of fission routes are discussed by model mechanisms, indicating that the size of the cage leads to plausible values of charge separation distances, as calculated from the experimental kinetic energy releases. It is also observed that boron undergoes massive hydrogen loss, whereas CH^+ remains intact in fission. Channels involving CH^+ appears to be more intense in some cases than the corresponding B^+ channels. This is taken as evidence that the carbon moieties are traps for the positive charges in doubly charged orthocarborane.

X-ray-induced and plasma-enhanced CVD are suitable methods to prepare semiconducting boron carbide films. The processes leading to these films have been discussed recently in the context of the singly charged fragment ions [15]. The present work clearly indicates that fission dominates in the soft X-ray regime above the B 1s-edge. These processes lead with high intensity to the loss of protons as well as the formation of the charged atomic fragments B^+ and CH^+. Correlated fragments of higher mass are clearly less important.

There are several implications for materials science that follow from the observed favorable fission process for orthocarborane above the core ionization thresholds. The inclusion of small fragments in the semiconducting boron carbide grown from the fragmentation of the *closo*-carboranes may help explain some of the unusual self doping that is observed in this unusual semiconductor [3, 8]. While synchrotron radiation initiated decomposition of the *closo*-carboranes will result in a semiconducting boron carbide, the resulting devices do not exhibit as good a figure of merit as those devices formed from materials resulting from the plasma enhanced decomposition of the *closo*-carboranes [10] or by decomposition of the *closo*-carboranes using soft X-rays well below the core ionization thresholds. These different boron carbides may in fact be different boron carbide polytypes, as a result of different abundances of the *closo*-carborane fragments.

Acknowledgements This work was financially supported by the Natural Sciences and Engineering Research Council of Canada, the National Science Foundation through grant CHE-0415421 and CHE-0650453, the Deutsche Forschungsgemeinschaft through grant RU 420/8-1, and the Fonds der Chemischen Industrie. We thank the staff of the Advanced Light Source (funded by DoE) and BESSY for their assistance. We thank Dr. Walter Braun (BESSY and Helmholtz-Centre Berlin for Materials and Energy) for his continuous encouragement and support of our work during the last decades.

References

[1] T. L. Heying, J. W. Ager, S. L. Clark, D. J. Mangold, H. L. Goldstein, M. Hillman, R. J. Polak, and J. W. Szymanski, Inorg. Chem. **2**, 1089 (1963).
H. Schroeder, T. L. Heying, and J. R. Reiner, Inorg. Chem. **2**, 1092 (1963).
T. L. Heying, J. W. Ager, S. L. Clark, R. P. Alexander, S. Papetti, J. A. Reid, and S. I. Trotz, Inorg. Chem. **2**, 1097 (1963).
S. Papetti and T. L. Heying, Inorg. Chem. **2**, 1105 (1963).
M. M. Fein, J. Bobinski, N. Mayes, N. Schwartz, and M. S. Cohen, Inorg. Chem. **2**, 1111 (1963).
M. M. Fein, D. Grafstein, J. E. Paustian, J. Bobinski, B. M. Lichstein, N. Mayes, N. N. Schwartz, and M. S. Cohen, Inorg. Chem. **2**, 1115 (1963).
D. Grafstein, J. Bobinski, J. Dvorak, H. Smith, N. Schwartz, M. S. Cohen, and M. M. Fein, Inorg. Chem. **2**, 1120 (1963).
D. Grafstein, J. Bobinski, J. Dvorak, J. E. Paustian, H. F. Smith, S. Karlan, C. Vogel, and M. M. Fein, Inorg. Chem. **2**, 1125 (1963).
D. Grafstein and J. Dvorak, Inorg. Chem. **2**, 1128 (1963).

[2] S.-D. Hwang, D. Byun, N. J. Ianno, P. A. Dowben, and H. R. Kim, Appl. Phys. Lett. **68**, 1495 (1996).
S.-D. Hwang, N. B. Remmes, P. A. Dowben, and D. N. McIlroy, J. Vac. Sci. Technol. B **14**, 2957 (1996).
S.-D. Hwang, K. Yang, P. A. Dowben, A. A. Ahmad, N. J. Ianno, J. Z. Li, J. Y. Lin, H. X. Jiang, and D. N. McIlroy, Appl. Phys. Lett. **70**, 1028 (1997).
S.-D. Hwang, N. Remmes, P. A. Dowben, and D. N. McIlroy, J. Vac. Sci. Technol. A **15**, 854 (1997).
D. N. McIlroy, S.-D. Hwang, K. Yang, N. Remmes, P. A. Dowben, A. A. Ahmad, N. J. Ianno, J. Z. Li, J. Y. Lin, and H. X. Jiang, Appl. Phys. A **67**, 335 (1998).
S. Balaz, D. I. Dimov, N. M. Boag, Kyle Nelson, B. Montag, J. I. Brand, and P. A. Dowben, Appl. Phys. A **84**, 149 (2006).
L. Carlson, D. LaGraffe, S. Balaz, A. Ignatov, Ya. B. Losovyj, J. Choi, P. A. Dowben, and J. I. Brand, Appl. Phys. A **89**, 195 (2007).
P. A. Dowben, O. Kizilkaya, J. Liu, B. Montag, K. Nelson, I. Sabirianov, and J. I. Brand, Mater. Lett. **63**, 72 (2009).

[3] A. N. Caruso, Ravi B. Billa, S. Balaz, Jennifer I. Brand, and P. A. Dowben, J. Phys.: Condens. Matter **16,** L139 (2004).

[4] B. W. Robertson, S. Adenwalla, A. Harken, P. Welsch, J. I. Brand, P. A. Dowben, and J. P. Claassen, Appl. Phys. Lett. **80**, 3644 (2002).

[5] B. W. Robertson, S. Adenwalla, A. Harken, P. Welsch, J. I. Brand, J. P. Claassen, N. M. Boag, and P. A. Dowben, in: Advances in Neutron Scattering Instrumentation, edited by I. S. Anderson and B. Guérard, Proc. SPIE **4785**, 226 (2002).

[6] S. Adenwalla, R. Billa, J. I. Brand, E. Day, M. J. Diaz, A. Harken, A. S. McMullen-Gunn, R. Padmanabhan, and B. W. Robertson, in: Penetrating Radiation Systems and Applications V, Proc. SPIE **5199**, 70 (2003).

[7] K. Osberg, N. Schemm, S. Balkir, J. I. Brand, S. Hallbeck, P. Dowben, and M. W. Hoffman, IEEE Sens. J. **6**, 1531 (2006).
K. Osberg, N. Schemm, S. Balkir, J. I. Brand, S. Hallbeck, and P. Dowben, in: Proc. 2006 IEEE International Symposium on Circuits and Systems (ISCAS 2006), p. 1179.

[8] A. N. Caruso, P. A. Dowben, S. Balkir, N. Schemm, K. Osberg, R. W. Fairchild, O. B. Flores, S. Balaz, A. D. Harken, B. W. Robertson, and J. I. Brand, Mater. Sci. Eng. B **135**, 129 (2006).

[9] E. Day, M. J. Diaz, and S. Adenwalla, J. Phys. D, Appl. Phys. **39**, 2920 (2006).
[10] D. Byun, B. R. Spady, N. J. Ianno, and P. A. Dowben, Nanostruct. Mater. **5**, 465 (1995).
[11] D. L. Schulz, A. Lutfurakhmanov, B. Maya, J. Sandstrom, D. Bunzow, S. B. Qadri, R. Q. Bao, D. B. Chrisey, and A. N. Caruso, J. Non-Cryst. Solids **354**, 2369 (2008).
[12] S. Lee, J. Mazurowski, G. Ramseyer, and P. A. Dowben, J. Appl. Phys. **72**, 4925 (1992).
S. Lee, T. Ton, D. Zych, and P. A. Dowben, Mater. Res. Soc. Symp. Proc. **283**, 483 (1993).
J. Mazurowski, S. Lee, G. Ramseyer, and P. A. Dowben, Mater. Res. Soc. Symp. Proc. **242**, 637 (1992).
S. Lee and P. A. Dowben, Appl. Phys. A **58**, 223 (1994).
D. Byun, S.-D. Hwang, P. A. Dowben, F. Keith Perkins, F. Filips, and N. J. Ianno, Appl. Phys. Lett. **64**, 1968 (1994).
[13] F. K. Perkins, M. Onellion, S. Lee, D. Li, J. Mazurowski, and P. A. Dowben, Appl. Phys. A **54**, 442 (1992).
[14] A. Yu. Ignatov, Ya. B. Losovyj, L. Carlson, D. LaGraffe, J. I. Brand, and P. A. Dowben, J. Appl. Phys. **102**, 083520 (2007).
[15] D. Feng, J. Liu, A. P. Hitchcock, A. L. D. Kilcoyne, T. Tyliszczak, N. Riehs, E. Rühl, J. D. Bozek, D. McIlroy, and P. A. Dowben, J. Phys. Chem. A **112**, 3311 (2008).
[16] A. P. Hitchcock, S. G. Urquhart, A. T. Wen, A. L. D. Kilcoyne, T. Tyliszczak, E. Rühl, N. Kosugi, J. D. Bozek, J. T. Spencer, D. N. McIlroy, and P. A. Dowben, J. Phys. Chem. B **101**, 3483 (1997).
[17] M. Simon, Ph.D. thesis, Université de Paris-Sud, Orsay (1992).
T. Lebrun, M. Lavollée, M. Simon, and P. Morin, J. Chem. Phys. **98**, 2534 (1993).
M. Simon, T. Lebrun, R. Martins, G. G. B. de Souza, I. Nenner, M. Lavollée, and P. Morin, J. Phys. Chem. **97**, 5228 (1993).
[18] E. Rühl, C. Heinzel, H. Baumgärtel, and A. P. Hitchcock, Chem. Phys. **169**, 243 (1993).
A. P. Hitchcock, M. J. McGlinchey, A. L. Johnson, W. K. Walter, M. Perez Jigato, D. A. King, D. Norman, E. Rühl, C. Heinzel, and H. Baumgärtel, J. Chem. Soc. Faraday Trans. **89**, 3331 (1993).
[19] E. Rühl, C. Schmale, H. W. Jochims, E. Biller, M. Simon, and H. Baumgärtel, J. Chem. Phys. **95**, 6544 (1991).
[20] E. Rühl, C. Heinzel, H. Baumgärtel, M. Lavollée, and P. Morin, Z. Phys. D **31**, 245 (1994).
[21] E. Rühl, Int. J. Mass Spectrom. **229**, 117 (2003).
[22] G. Dujardin, D. Winkoun, and S. Leach, Phys. Rev. A **31**, 3027 (1985).
G. Dujardin, L. Hellner, D. Winkoun, and M. J. Besnard, Chem. Phys. **105**, 291 (1986).
[23] J. H. D. Eland, Mol. Phys. **61**, 725 (1987).
J. H. D. Eland, Acc. Chem. Res. **22**, 281 (1989).
[24] E. Rühl, S. D. Price, S. Leach, and J. H. D. Eland, Int. J. Mass Spectrom. Ion. Proc. **97**, 175 (1990).
[25] A. P. Hitchcock, J. J. Neville, A. Jürgensen, and R. G. Cavell, J. Electron Spectrosc. Rel. Phenom. **88**, 71 (1998).
[26] W. C. Wiley and I. H. McLaren, Rev. Sci Instrum. **26**, 1150 (1955).
[27] J. Geiger and E. Rühl, Int. J. Mass Spectrom. Ion. Process. **220**, 99 (2002).
[28] B. Langer, N. Berrah, A. Farhat, O. Hemmers, and J. D. Bozek, Phys. Rev. A **53**, R1946 (1996).
[29] S. Bernstorff, W. Braun, M. Mast, W. Peatman, and T. Schroeter, Rev. Sci. Instrum. **60**, 2097 (1989).
[30] I. Last, I. Schek, and J. Jortner, J. Chem. Phys. **107**, 6685 (1997).
I. Last, Y. Levy, and J. Jortner, Proc. Natl. Acad. Sci. **99**, 9107 (2002).
I. Last, Y. Levy, and J. Jortner, Mol. Phys. **104**, 1227 (2006).
[31] S. Tobita, S. Leach, H. W. Jochims, E. Rühl, E. Illenberger, and H. Baumgärtel, Can. J. Phys. **70**, 1060 (1994).
[32] P. Scheier, B. Dünser, R. Wörgötter, M. Lezius, R. Robl, and T. D. Märk, Int. J. Mass Spectrom. Ion Process. **138**, 77 (1994).
[33] M. Thomas, 'Optical Grapher Program', Center of X-Ray Optics, U.C. Berkeley.
[34] R. C. Weast (ed.), Handbook of Chemistry and Physics, 63rd edition (CRC Press, Boca Raton, 1982).
[35] L. S. Cederbaum, J. Zobeley, and F. Tarantelli, Phys. Rev. Lett. **79**, 4778 (1997).
J. Zobeley, R. Santra, and L. S. Cederbaum, J. Chem. Phys. **115**, 5076 (2001).
[36] S. Marburger, O. Kugeler, U. Hergenhahn, and T. Möller, Phys. Rev. Lett. **90**, 203401 (2003).
[37] J. Berkowitz, Photoabsorption, Photoionization and Photoelectron Spectroscopy (Academic, New York, 1979).
[38] D. M. Curtis and J. H. D. Eland, Int. J. Mass Spectrom. Ion. Process. **63**, 241 (1985).